PHYSICAL REVIEW D **94,** 115016 (2016)

MSSM without free parameters

Ryuichiro Kitano,[1,2] Ryuji Motono,[1,2] and Minoru Nagai[3]

[1]*Institute of Particle and Nuclear Studies, High Energy Accelerator Research Organization (KEK), Tsukuba 305-0801, Japan*

[2]*The Graduate University for Advanced Studies (Sokendai), Tsukuba 305-0801, Japan*

[3]*Maskawa Institute for Science and Culture, Kyoto Sangyo University, Kyoto 603-8555, Japan*

(Received 4 August 2016; published 12 December 2016)

It is often argued that the minimal supersymmetric standard model has $O(100)$ free parameters, and the generic parameter region is already excluded by the null observation of the flavor and CP-violating processes as well as the constraints from the LHC experiments. This situation naturally leads us to consider the case where all the dangerous soft supersymmetry breaking terms, such as the scalar masses and scalar couplings, are absent, while only the unified gaugino mass term and the μ term are nonvanishing at the grand unification scale. We revisit this simple situation taking into account the observed Higgs boson mass, 125 GeV. Since the gaugino mass and the μ term are fixed in order to explain the Higgs boson and the Z boson masses, there is no free parameter left in this scenario. We find that there are three independent parameter sets that exist including ones which have not been discussed in the literature. We also find that the abundance of the dark matter can be explained by relic gravitinos which are nonthermally produced as decay products of the supersymmetry particles while satisfying constraints from big bang nucleosynthesis. We discuss the effects of the gravity mediation which generically gives a contribution to the soft terms of the order of the gravitino mass. It turns out that a newly found parameter set is preferable to explain the Higgs boson mass as well as the gravitino dark matter while satisfying the constraints from the electric dipole moments of the electron and the nucleon.

DOI: 10.1103/PhysRevD.94.115016

I. INTRODUCTION

The Higgs boson mass 125 GeV suggests that the physics behind the electroweak symmetry breaking is weakly coupled, but it is not quite as light as the predictions of TeV scale supersymmetry. In order to explain the Higgs boson mass in the minimal supersymmetric standard model (MSSM), the superpartner masses, especially the scalar top quarks, need to be above $\mathcal{O}(10)$ TeV in a generic region of the parameter space [1–4].

In light of this situation, models with the $\mathcal{O}(\mathrm{PeV})$ scale rather than the $\mathcal{O}(10)$ TeV supersymmetry have been discussed quite extensively [5–8]. (For earlier studies, see [9–12].) The reason for this jump from TeV to PeV is based on the constraints from the flavor- and CP-violating processes [13–15]. For example, the constraint from the CP violation in the kaon mixing provides us a bound of the order of PeV when the CP phase and the flavor mixing are $\mathcal{O}(1)$ in the sfermion sector. The PeV supersymmetry can (almost) avoid the flavor/CP constraints, while the dark matter of the Universe can be explained by the thermal relic of the light gauginos, in particular, the wino [16], whose masses can be suppressed by a one-loop factor (and, thus, the TeV scale) as in the anomaly mediation scenario [9,17].

On the other hand, the $\mathcal{O}(10)$ TeV supersymmetry, which is implied by the Higgs boson mass, requires a nongeneric feature in the flavor structures of the superparticles. For example, there have been proposals to achieve such structures by a flavor-blind mechanism for supersymmetry breaking and its transmission to the visible sector [18–21]. In any case, since we need some mechanism to suppress large flavor and CP violations, the gravity-mediated contributions which generically break flavor and CP should be suppressed; i.e., the gravitino should be much lighter than other supersymmetry (SUSY) particles. In this case, the gravitino can be a good candidate of the dark matter; its abundance may be explained by the decay of other SUSY particles which are thermally produced [22,23].

In this paper, we discuss the scenario where all SUSY breaking parameters, except gaugino mass, are set to be zero at the cutoff scale, and, thus, the severe flavor and CP constraints can be alleviated. Such a setup has been studied as the low energy effective theory of the gaugino mediation scenario [20,21] or the no-scale supergravity Lagrangian [24,25]. The right-handed stau tends to be the next-to-lightest SUSY particle (NLSP), and its decay into the gravitino may explain the observed dark matter abundance. However, it is nontrivial whether the Higgs boson mass and dark matter abundance can be explained simultaneously in this simple setup. The large stau mass is required to avoid the severe constraints from big bang nucleosynthesis (BBN), while stop masses are bounded from above according to the value of $\tan\beta$ to explain the observed Higgs boson mass.

We discuss the running behavior of the Higgs B term carefully and find that a new parameter set with relatively small $\tan\beta$ appears for a large SUSY breaking scale even with a vanishing Higgs B term at the cutoff scale. This helps to solve the above-mentioned tension; small $\tan\beta$ enlarges the right-handed stau mass and also relaxes the upper bound on the stop masses. The small gravity-mediated contributions can become the sources of flavor and CP violation in the model. However, we find that thanks to the small value of $\tan\beta$, the predicted electron electric dipole moment (EDM) is marginal to the present experimental bound and should be checked in the near-future experiments.

This paper is organized as follows. In Sec. II, we explain our model to solve the SUSY flavor and CP problems. The renormalization group running of the Higgs B term is examined carefully, and we identify the parameter regions with the correct electroweak symmetry breaking (EWSB) minimum. The spectrum of SUSY particles and the lightest Higgs boson are also presented here. We discuss the implications on the gravitino dark matter in Sec. III and predictions of the electron and nucleon EDMs in Sec. IV. In Sec. V, we discuss the thermal component of the gravitino relic abundance. We summarize our results in Sec. VI.

II. *CP*- AND FLAVOR-SAFE MINIMAL SUSY MODEL

In the MSSM, independent CP phases are expressed in the combination of the A term, B term, μ term, and gaugino masses M_i,

$$\phi_{\mu,i} = \arg(M_i \mu(-B\mu)^*), \quad \phi_{A_f,i} = \arg(M_i A_f^*), \quad (f = u,d,e). \tag{1}$$

Usually, we take the basis with real $B\mu$ by the appropriate redefinitions of fields so that the vacuum expectation values (VEVs) of the two Higgs doublets become real. Flavor and CP violations come from the off-diagonal terms of the sfermion mass terms in the super Cabibbo-Kobayashi-Maskawa basis,

$$\left(m_{\tilde{f}}^2\right)_{ij}, \qquad (i \neq j). \tag{2}$$

If the SUSY scale is below 100 TeV, random values of these parameters predict detectable flavor-changing neutral current (FCNC) and CP-violating phenomena.

We assume that all A terms, B terms, and sfermion soft masses vanish at some scales,

$$A_{u,d,e} = B = m^2_{\tilde{q},\tilde{u},\tilde{d},\tilde{l},\tilde{e}} = 0. \tag{3}$$

At the low energy scale, the nonvanishing A and B terms are generated by the radiative corrections through the gauge interactions. Since these contributions are proportional to gaugino masses, there appear no CP phases at the low energy scale as long as the phases of the three gaugino mass parameters are aligned. The off-diagonal elements of sfermion mass are also generated only radiatively through the Cabibbo-Kobayashi-Maskawa matrix, and the flavor constraints can become rather weak. The remaining free parameters are Higgs soft masses and gaugino masses,

$$m^2_{H_u}, \qquad m^2_{H_d}, \qquad M_{1,2,3}. \tag{4}$$

We consider the minimal situation where the SUSY breaking is directly mediated only to the gauge sectors by the physics of grand unification theories (GUTs). Then, we further impose the following conditions at the GUT scale $M_{\rm G}$,

$$m^2_{H_u} = m^2_{H_d} = 0, \qquad M_1 = M_2 = M_3 = M_{1/2}. \tag{5}$$

In this way, one can consider a very predictive framework where we have only one SUSY breaking parameter $M_{1/2}$ and one supersymmetric parameter μ. Here, we do not discuss a specific mechanism for generating the μ term as a result of supersymmetry breaking; i.e., we do not try to solve the μ problem. As the simplest but consistent model, we consider the case where the μ parameter is just present as a term in the superpotential. Note here that there is no CP-violating phase in this scenario as long as we set $A = 0$ and $B = 0$ at the unification scale; i.e., the μ parameter can be taken to be real without loss of generality. The size of the SUSY breaking is naively estimated as $M_{1/2} \simeq \mathcal{O}(F/M_{\rm G})$, and, thus, the gravitino becomes the lightest SUSY particle with mass $m_{3/2} = F/(\sqrt{3}M_{\rm pl}) \simeq 10^{-(2-3)} M_{1/2}$. The small gravitino mass is also favored to suppress the possibly dangerous gravity-mediated contributions, which are the main sources of flavor and CP violations in our scenario.

In this model, the ratio of the VEVs $\tan\beta = \langle H_u\rangle/\langle H_d\rangle$ is not a free parameter and is determined by the condition of the EWSB. At the SUSY scale $\mathcal{O}(10)$ TeV, the following conditions should be imposed:

$$\frac{m_Z^2}{2} = -|\mu|^2 + \frac{m^2_{H_u} + \Sigma_u}{\cot^2\beta - 1} - \frac{m^2_{H_d} + \Sigma_d}{1 - \tan^2\beta}, \tag{6}$$

$$\sin 2\beta = -\frac{B\mu}{2|\mu|^2 + m^2_{H_u} + m^2_{H_d} + \Sigma_u + \Sigma_d}, \tag{7}$$

where $\Sigma_{u,d}$ includes the tadpole contributions that originated from the one-loop corrections.[1] For a given choice of $M_{1/2}$, these two constraints fix the μ parameter as well as the value of $\tan\beta$ by requiring that the B parameter vanish

[1]Here, we use the one-loop effective potential to determine only μ, β, and masses of heavy Higgs bosons. On the other hand, the lightest Higgs boson mass is calculated by the effective field theory approach following [4,26,27] since we consider a relatively high SUSY scale to explain the observed Higgs boson mass.

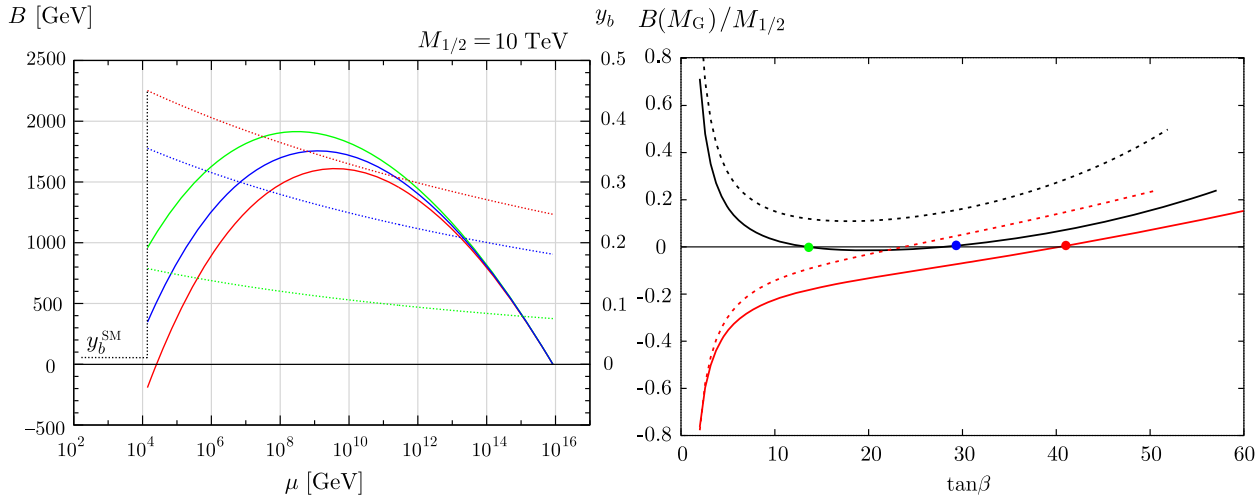

FIG. 1. Left: The running behaviors of the Higgs B parameter (solid lines with left y axis) and the bottom Yukawa couplings (dotted lines with right y axis) for $M_{1/2} = 10$ TeV. Each colored line corresponds to the solution with (I) $\mu > 0$ (red), (II) $\mu < 0$ with large $\tan\beta$ (blue), and (III) $\mu < 0$ with small $\tan\beta$ (green). Right: The values of the B parameter at the GUT scale as a function of $\tan\beta$. The red (black) lines correspond to the solution with $\mu > 0$ ($\mu < 0$). The B parameters are normalized by $M_{1/2}$, and the dotted (solid) lines correspond to the case for $M_{1/2} = 1(10)$ TeV. The red, blue, and green dots correspond to the three solutions I, II, and III for $M_{1/2} = 10$ TeV.

at the unification scale. We choose $0 < \beta < \pi/2$ to obtain positive VEVs of two Higgs doublets. In this convention, the sign of the B term determines that of the μ term. The low energy value of the B parameter is evaluated by the following renormalization group (RG) equation,[2]

$$16\pi^2 \frac{dB}{d\log\mu} \simeq -3g_2^2 M_2 - g_1^2 M_1 + y_\tau^2 A_\tau + 3y_b^2 A_b + 3y_t^2 A_t. \tag{8}$$

Here, the bottom Yukawa coupling receives sizable threshold corrections for large $\tan\beta$, and its value is sensitive to the size of $\tan\beta$ and the sign of μ,

$$y_b(\mu_{\rm SUSY}) \simeq \frac{g_2 m_b}{\sqrt{2} m_W} \frac{\tan\beta}{1+\varepsilon_b \tan\beta}, \qquad \varepsilon_b \approx \frac{\alpha_s}{3\pi}\frac{\mu M_3}{m_{\tilde{q}}^2}. \tag{9}$$

The typical running behaviors of the B parameter and the bottom Yukawa coupling are presented in Fig. 1 (left). At a high energy scale, the B parameter is increased by the gauge interactions as the renormalization scale μ goes down. Since the values of the A terms are also enhanced at the low energy scale, the B parameter turns to be decreased by the Yukawa interactions. We find three solutions to satisfy the EWSB conditions,

(I) $\mu > 0$, $B < 0$, and large $\tan\beta$;
(II) $\mu < 0$, $B > 0$, and large $\tan\beta$;
(III) $\mu < 0$, $B > 0$, and small $\tan\beta$.

In scenario I, the values of y_b and $\tan\beta$ are large enough to drive the B parameter negative. The large $\tan\beta$ implies a small absolute value of the B parameter according to Eq. (7). For smaller but still large y_b, the B parameter stays positive even at the SUSY scale, and its absolute value is small in scenario II. For much smaller y_b, we obtain a large B parameter, implying small $\tan\beta$ in scenario III. We note that the large B parameter is preferable to suppress CP phases generated by the gravity-mediated contributions, which are estimated as $\phi_\mu \sim m_{3/2}/|B|$.

The solutions II and III do not appear when the SUSY scale is low since the contributions from Yukawa couplings are quite effective in the low energy region, always resulting in a negative B parameter. In Fig. 1 (right), we show the values of the B parameter at the GUT scale as functions of $\tan\beta$ for $M_{1/2} = 1$ and 10 TeV. For large $\tan\beta$, the B parameter has to be large enough at the GUT scale to have small absolute value at the SUSY scale since it receives large negative contributions coming from the large bottom Yukawa coupling. Then, we always have a solution of $B(M_{\rm G}) = 0$ for $\mu > 0$ (red lines) irrespective of $M_{1/2}$. On the other hand, the solutions with $\mu < 0$ (black lines) appear only for large $M_{1/2}$ since the negative contributions of the Yukawa couplings are weakened for the high SUSY scale.

This argument shows that the appearance of parameter regions with $\mu < 0$ is sensitive to the precise sizes of Yukawa couplings and also to the GUT scale $M_{\rm G}$. We take the GUT scale as the scale with $g_1(M_{\rm G}) = g_2(M_{\rm G})$, which becomes a little bit smaller for the higher SUSY scale. The precise value of the top Yukawa couplings is also essential to calculate the Higgs boson mass in the SUSY model. Therefore, in the following analysis, we take a relatively large uncertainty for the top pole mass $M_t = 173.3 \pm 2$ GeV compared to the result obtained by the LHC

[2]In the actual calculation of the SUSY spectrum, we use two-loop renormalization group equations above the SUSY scale.

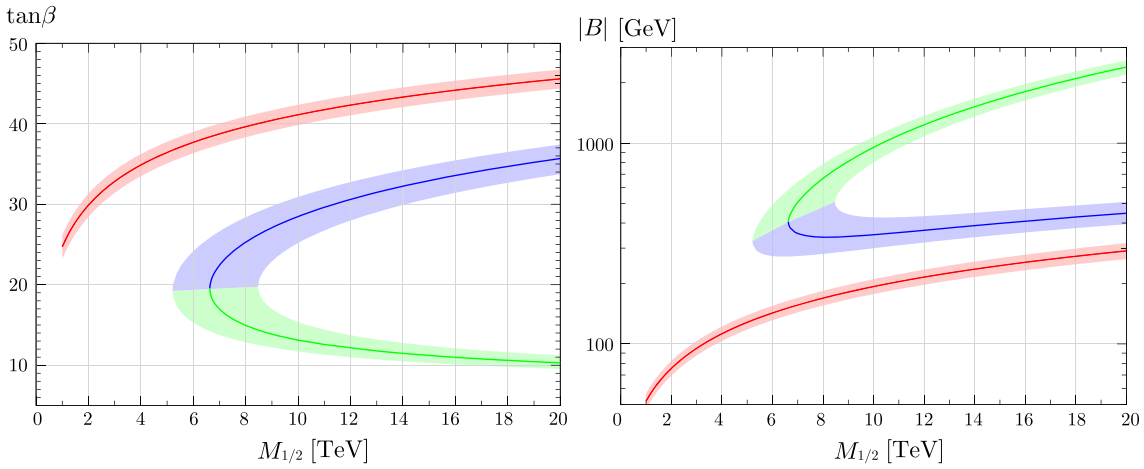

FIG. 2. The values of $\tan\beta$ (left) and $|B|$ (right) as a function of $M_{1/2}$. The red, blue, and green lines correspond to scenarios I, II and III respectively. The colored bands show the uncertainty coming from the top mass, $M_t = 173.3 \pm 2$ GeV.

experiments [28–30], taking into account the possible difference between the measured mass parameter and the pole mass. Also, since we are focusing on high-scale SUSY models, we adapt the effective field theory approach to calculate the lightest Higgs boson mass. Concretely, we use three-loop Standard Model (SM) RG equations to calculate the Yukawa couplings at the SUSY scale ($\sim M_{1/2}$) and to obtain a Higgs quartic coupling at the SM scale ($\sim M_t$).

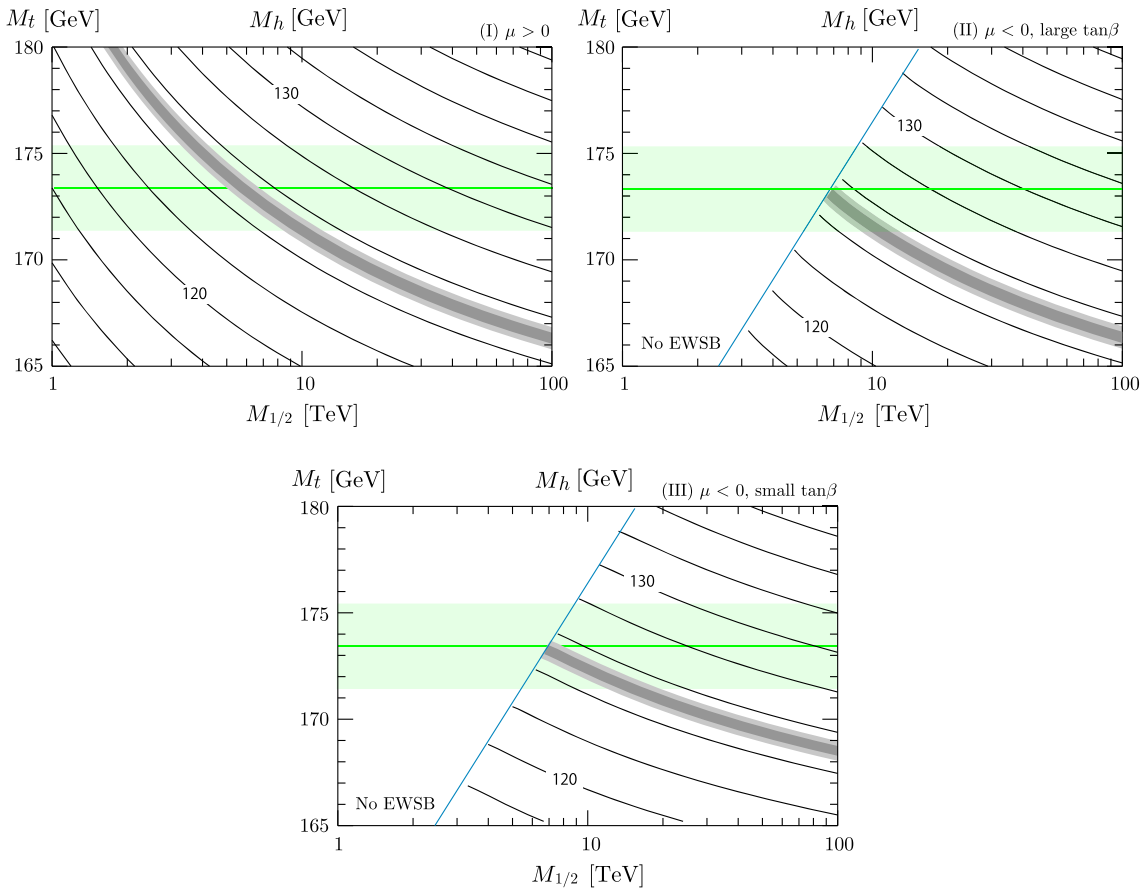

FIG. 3. Contour plots for the mass of the Higgs boson as functions of $M_{1/2}$ and M_t in scenario I (top left), II (top right), and III (bottom). Gray shaded regions are favored by the measurements of the Higgs boson mass by the LHC experiments. Green regions indicate the uncertainty of the top mass.

Appropriate threshold corrections are included according to [4,26,27] both at the EW scale and at the SUSY scale. The SUSY spectrum is calculated by solving two-loop RG equations.[3] Here, we stress again that our model now has only one parameter $M_{1/2}$ that can be determined uniquely for each of the solutions, I, II, and III to reproduce the observed Higgs boson mass 125 GeV up to the current experimental uncertainties in the determinations of the Higgs boson mass and the top quark mass as well as the theoretical uncertainties in the calculations of the mass spectrum of the superparticles.

In Fig. 2, we show the values of $\tan\beta$ and $|B|$ at the SUSY scale for each solution. In the case of solutions I and II, $\tan\beta$ is a monotonically increasing function of $M_{1/2}$. This is because negative contributions from the top Yukawa coupling are weakened for the large SUSY scale, and the bottom Yukawa coupling has to be larger to obtain small $|B|$. On the other hand, $\tan\beta$ becomes smaller for large $M_{1/2}$ in the case of solution III, simply because we obtain larger $|B|/M_{1/2}$ for larger $M_{1/2}$ due to the smaller contributions from Yukawa couplings, and it implies smaller $\tan\beta$ according to Eq. (7). The obtained size of $|B|$ is about $\mathcal{O}(100)$ GeV, which is much smaller than $M_{1/2} \sim 10$ TeV because of the large cancellation between gauge interactions and Yukawa interactions. However, $|B|$ could be large enough $|B| \gtrsim 1$ TeV in the case of solution III because negative contributions from Yukawa couplings are weakened thanks to the high SUSY scale and the low value of $\tan\beta$.

In Fig. 3, we show the parameter regions which explain the correct Higgs boson mass, $m_h = 125.09 \pm 0.24$ GeV [32], in the $(M_{1/2}, M_t)$ plane for scenarios I (top left), II (top right), and III (bottom). Because of the uncertainty of the top mass, $M_{1/2}$ is not determined uniquely, and instead we obtain an upper and lower bound on it. For solution I, the observed Higgs boson can be explained in the range of 3.5 TeV $\lesssim M_{1/2} \lesssim$ 12 TeV depending on the top mass. In the case of solutions II and III, the SUSY scale has to be large enough to realize the EWSB, and also a little bit larger $M_{1/2}$ is required for solution III since $\tan\beta$ is relatively small. We find 6.5 TeV $\lesssim M_{1/2} \lesssim$ 13 TeV for solution II and 6.5 TeV $\lesssim M_{1/2} \lesssim$ 20 TeV for solution III. We find that the top mass should be less than 174 GeV in scenarios II and III. As the top mass becomes smaller, a larger $M_{1/2}$ is necessary to have enough radiative corrections to the Higgs mass. In particular, the required $M_{1/2}$ is increased rapidly in solution III since the tree-level contributions to the Higgs mass, which is proportional to $\cos 2\beta$, are also decreased for larger $M_{1/2}$. This figure shows that the precise measurements of the masses of the top quark and the Higgs boson are essential to confirm or exclude our model.

Since our model contains only one SUSY breaking scale which is much larger than the EW scale, most SUSY parameters are roughly proportional to $M_{1/2}$. Typical SUSY parameters for each solution are presented in Table I. The NLSP particle is the right-handed stau, which decays to the LSP gravitino dark matter. Stau mass is rather sensitive to $\tan\beta$, i.e., the tau Yukawa coupling, since the flavor-independent contribution from gauge interactions is smaller than other sfermion mass terms. In the case of solution I, the right-handed stau mass is much smaller than the selectron mass since the tau Yukawa coupling is effective. The mass difference between the stau and the selectron becomes smaller for solution II and they are almost degenerate in the case of solution III. This means that the right-handed stau gets heavier in solution III compared to the other solutions for a fixed $M_{1/2}$, as shown in Fig. 4. In the last row of Table I, we present the gravitino mass which explains the observed dark matter abundance by the decay of other SUSY particles, as will be explained

TABLE I. Typical mass parameters in each scenario. In the last row, we present the expected mass of the gravitino which explains the whole observed dark matter abundance through the production by the decay of other SUSY particles.

	I ($\mu > 0$)	II ($\mu < 0$)	III ($\mu < 0$)
M_t(GeV)	173.3	172.0	172.0
$M_{1/2}$(TeV)	5.0	10.0	15.0
$\tan\beta$	36.5	30.3	10.5
B(GeV)	−127	312	1776
M_h(GeV)	124.5	125.4	125.6
M_A(TeV)	4.85	9.29	15.5
M_1(TeV)	2.30	4.73	7.21
M_2(TeV)	4.05	8.19	12.4
M_3(TeV)	9.65	18.6	27.3
μ(TeV)	4.64	−8.38	−12.1
$m_{\tilde{e}_R}$(TeV)	1.80	3.58	5.35
$m_{\tilde{\tau}_R}$(TeV)	1.39	3.17	5.27
$m_{\tilde{e}_L}$(TeV)	3.16	6.22	9.24
$m_{\tilde{\tau}_L}$(TeV)	3.06	6.11	9.22
$m_{\tilde{u}_R}$(TeV)	8.08	15.3	22.3
$m_{\tilde{t}_R}$(TeV)	6.84	13.1	19.0
$m_{\tilde{d}_R}$(TeV)	8.02	15.2	22.1
$m_{\tilde{b}_R}$(TeV)	7.64	14.6	22.0
$m_{\tilde{u}_L}$(TeV)	8.50	16.2	23.6
$m_{\tilde{t}_L}$(TeV)	7.76	14.9	22.1
A_u (TeV)	9.22	17.3	25.0
A_t (TeV)	7.33	14.0	20.7
A_d (TeV)	10.3	19.4	29.0
A_b (TeV)	9.26	17.6	27.5
A_e (TeV)	2.16	4.42	7.65
A_τ (TeV)	1.96	4.21	7.61
$m_{3/2}^{\mathrm{NT}}$(GeV)	509	179	76

[3]We compared our results with those obtained by a modified version of SOFTSUSY [31], which reproduces the gauge and Yukawa couplings derived by the effective field approach at the high energy scale, and we found that the difference of the obtained SUSY masses is within 1%.

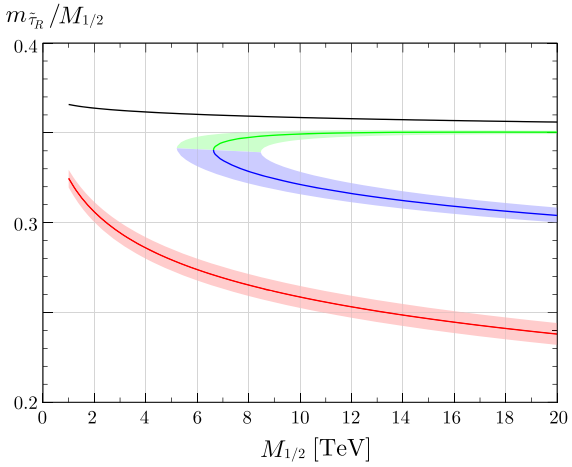

FIG. 4. The right-handed stau mass normalized by $M_{1/2}$ as a function of $M_{1/2}$ in scenarios I (red), II (blue), and III (green). The black line represents the selectron mass normalized by $M_{1/2}$.

in detail in the next section. This gravitino mass is roughly inversely proportional to $M_{1/2}$.

III. GRAVITINO DARK MATTER

As is explained in the Introduction, the gravitino mass is assumed to be small to suppress the gravity-mediated contributions. Thus, the gravitino can be a good dark matter candidate in this model.

We assume that the NLSP stau is produced thermally in the history of the Universe, and its thermal relic abundance reads as

$$\Omega_{\tilde{\tau}_R}h^2 \approx \frac{1.1\times 10^9\ \mathrm{GeV}^{-1}}{\sqrt{g_\star}m_{\mathrm{pl}}\langle\sigma v\rangle x_f} \approx 0.17\left[\frac{10}{\sqrt{g_\star}}\right]\left[\frac{1/20}{x_f}\right]\left[\frac{10^{-9}\ \mathrm{GeV}^{-2}}{\langle\sigma v\rangle}\right], \quad (10)$$

where $g_\star$ is the effective number of relativistic degrees of freedom at the freeze-out temperature T_f, $x_f = T_f/m_{\tilde{\tau}_R}$, and $m_{\mathrm{pl}} = \sqrt{8\pi}M_{\mathrm{pl}} = 1.22\times 10^{19}$ GeV. The right-handed staus mainly annihilate into the gauge boson pairs $\tilde{\tau}\tilde{\tau}^* \to \gamma\gamma$, γZ, ZZ, WW, and also they annihilate into the tau lepton pairs through the bino exchange, $\tilde{\tau}\,\tilde{\tau} \to \tau\tau$ [33]. Furthermore, since we find that the contribution through the left-right mixing described below cannot be neglected for the large $\tan\beta$ case, we include the effects as denoted by y_{eff}. Then the thermally averaged annihilation cross section of the right-handed staus is estimated as[4]

$$\langle\sigma v\rangle \simeq \frac{\pi\alpha^2}{m_{\tilde{\tau}_R}^2}\left[1+2t_W^2+\left\{t_W^4+\frac{(1-y_{\mathrm{eff}}^2)^2}{32c_W^4}\right\}+\frac{(1-y_{\mathrm{eff}}^2)^2}{16c_W^4}\right] + \frac{8\pi\alpha^2M_B^2}{c_W^4(m_{\tilde{\tau}_R}^2+M_B^2)^2}. \quad (11)$$

Each term in the square bracket of the first term corresponds to the contributions from $\gamma\gamma$, $Z\gamma$, ZZ, and WW final states, respectively, and the last term is the contribution from the $\tau\tau$ mode. Here, $c_W = \cos\theta_W$, $t_W = \tan\theta_W$, and y_{eff} stands for the term proportional to the tau Yukawa coupling,

$$y_{\mathrm{eff}} = \frac{\mu}{\sqrt{m_{\tilde{\tau}_R}^2+m_{\tilde{\tau}_L}^2}}\frac{m_\tau\tan\beta}{t_W m_W(1+\varepsilon_\tau\tan\beta)}, \quad (12)$$

where ε_τ is the threshold corrections to the tau Yukawa coupling and $\varepsilon_\tau \simeq -3\alpha_2/(16\pi)\mu M_2/m_{\tilde{\tau}_R}^2$ for degenerate SUSY masses. This term is generated by the mixing effect between the left-handed and right-handed staus, it becomes relevant for large $\tan\beta$, and it does not decouple in the limit of the large SUSY scale as one can see from the formula. In particular, it can remain significant in the limit of small left-right mixing θ_τ, which is suppressed by the heavy SUSY mass, $\theta_\tau \simeq \mathcal{O}(m_\tau\tan\beta/m_{\mathrm{SUSY}})$. In scenarios I and II, y_{eff} can be much larger than $\sqrt{2}$, and, thus, the annihilation cross sections are enhanced. Especially in scenario I, the enhancement is as large as 50% compared with the case of ignoring the left-right mixing. In the case of scenario III where $\tan\beta$ is small, the cross section tends to be slightly decreased by considering nonvanishing y_{eff}. On the contrary, the enhancements of the annihilation into the hh [37] and tt [38] final states are irrelevant for us since they require both large $\tan\beta$ and large θ_τ.

The gravitinos are generated nonthermally through the decay of the staus. The relic density of the gravitino dark matter is given as

$$\Omega_{\tilde{G}}^{\mathrm{NT}}h^2 = \frac{m_{3/2}}{m_{\tilde{\tau}_R}}\Omega_{\tilde{\tau}_R}h^2. \quad (13)$$

The minimal scenario is to consider that the observed cold dark matter density $\Omega_c h^2 = 0.12$ [39] is explained by the gravitino dark matter produced in this way. Thus, we can predict the gravitino mass as $m_{3/2}^{\mathrm{NT}} = m_{\tilde{\tau}_R}\Omega_c/\Omega_{\tilde{\tau}_R}$, which is roughly inversely proportional to the right-handed stau mass from Eqs. (10) and (11). In Fig. 5 (left), we show the predicted masses of gravitino dark matter for each scenario. We find the gravitino masses sit in the right parameter range anticipated by a naive estimation $m_{3/2}/M_{1/2} \approx \mathcal{O}(M_{\mathrm{G}}/M_{\mathrm{pl}}) \simeq \mathcal{O}(0.01)$, and it gives the strong implication on the concrete ultraviolet model construction. In scenario III, the gravitino can become relatively light, below 100 GeV for $M_{1/2} > 12$ TeV, since

[4]Here we show only S-wave contributions and drop the terms suppressed by $\tan\beta$ and/or m_{SUSY}. In the numerical calculation, we include remaining minor decay channels and solve the Boltzmann equations to include both the coannihilation effects and P-wave contributions according to [34,35]. We have checked that Sommerfeld effects discussed in [36] give only negligible modifications in our setup.

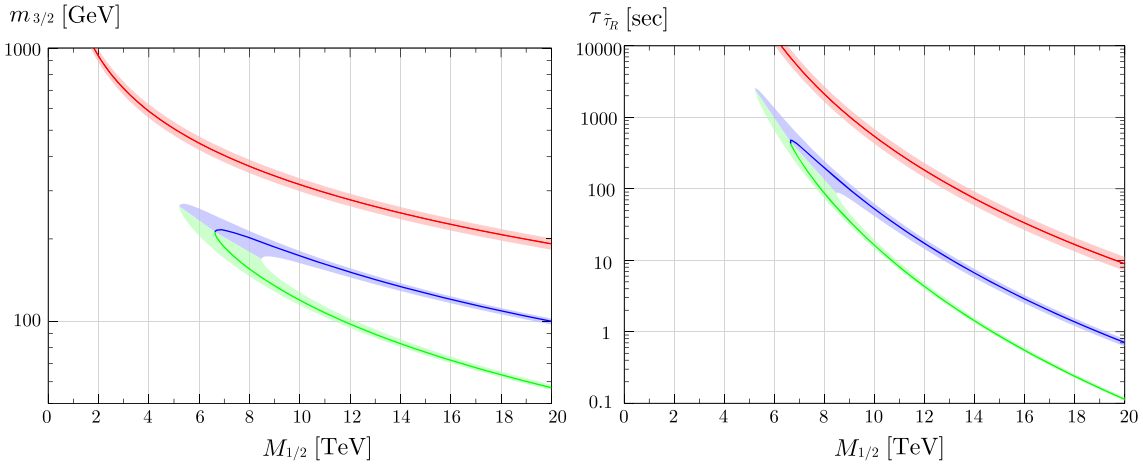

FIG. 5. The predicted mass of the gravitino LSP (left) and the lifetime of the right-handed stau NLSP (right) as functions of $M_{1/2}$ for scenarios I (red), II (blue), and III (green). Here, the gravitino dark matter is assumed to be mainly produced by the decay of other SUSY particles and becomes the dominant component of the cold dark matter in our Universe.

the right-handed stau mass tends to be heavy due to the small $\tan\beta$. In the following, we will see that light gravitinos are favored by the constraints from the BBN and also from the EDM experiment. Then, in scenarios I and II, the entire dark matter cannot be identified as nonthermally produced gravitinos, and we must consider other production mechanisms and/or other dark matter candidates. In a later section, we will consider the case where gravitinos are also thermally produced in the early stage of the Universe and discuss the implications on the reheating temperature after inflation.

Next, we consider the BBN constraints on this model. Since the lifetime of the stau NLSP is relatively long in our model, its late-time decay may destroy the successful predictions of the standard BBN scenario [40,41]. The stau lifetime is estimated as

$$\tau_{\tilde{\tau}_R} \simeq \frac{48\pi m_{3/2}^2 M_{\rm pl}^2}{m_{\tilde{\tau}_R}^5} \simeq 10 \text{ sec} \left(\frac{m_{3/2}}{100 \text{ GeV}}\right)^2 \left(\frac{m_{\tilde{\tau}_R}}{3 \text{ TeV}}\right)^{-5}. \tag{14}$$

For $\tau_{\tilde{\tau}_R} < 1$ sec, the NLSP stau can decay before the BBN starts. For 1 sec $< \tau_{\tilde{\tau}_R} < 100$ sec, the hadronic particles produced by the NLSP decay are potentially dangerous since they interconvert the protons and neutrons and may change the helium abundance. Especially in the stau NLSP case, since the staus mainly decay to the tau lepton and gravitino pairs $\tilde{\tau}_R \to \tilde{G}\tau$, sizable amounts of pions are produced through the hadronic decay of tau leptons. However, the produced pions are less effective to interconvert the protons and neutrons than the $p\bar{p}$ and $n\bar{n}$ pairs. From the figures of [42], we find that the stau abundance considered here is not problematic. Although these analyses are performed for lower stau masses, produced taus are stopped immediately with losing their energy electromagnetically, and, therefore, the constraint is less sensitive to the stau mass itself in this time range. On the other hand, the case with $\tau_{\tilde{\tau}_R} > 100$ sec is excluded by the overproduction of D as one can see from Ref. [42]. Then, in the following, we assume that thermally produced NLSP staus are allowed as long as $\tau_{\tilde{\tau}_R} < 100$ sec, and clearly more detailed analyses of BBN constraints on heavy NLSP masses are desirable.

We show the stau lifetime as a function of $M_{1/2}$ in Fig. 5 (right). Comparing with the predictions of the Higgs mass (Fig. 3), we can conclude that the parameter region explaining the correct Higgs mass is in tension with the BBN constraint in scenario I. In scenario II, we need $M_{1/2} \gtrsim 9$ TeV, and the top quark mass is preferably a little bit smaller than the currently measured central value, and a further wider parameter region survives in scenario III.

IV. ELECTRIC DIPOLE MOMENTS

Although we assume the favor- and CP-safe condition Eq. (3) at the tree level, the additive gravity mediation effects of the order of the gravitino mass are not negligible in our model if the abundance of the gravitino dark matter is explained by the decay of NLSP stau particles. Such gravity-mediated contributions become new sources of the flavor and CP violation.

For $m_{3/2} \sim 100$ GeV and $m_{\rm SUSY} \sim 10$ TeV, as in the case of scenarios II and III, the size of the flavor mixing is suppressed as

$$m_{3/2}^2/m_{\rm SUSY}^2 \sim \mathcal{O}(10^{-4}). \tag{15}$$

The constraints from the FCNC processes, such as the kaon mixing and $\mu \to e\gamma$, can be satisfied for such a small mixing as well as heavy sfermion masses [13–15]. The most important signature of the model is the flavor diagonal

CP-violating phenomena, i.e., the EDMs of the electron and the nucleon.[5]

The CP violation arises from the mismatch of the phase in the two different contributions to the B term, i.e., from the gravity mediation effects of $\mathcal{O}(m_{3/2})$ and from the radiatively generated B term of $\mathcal{O}(\alpha M_{1/2})$. As we discussed in Eq. (1), the mismatch causes a nonvanishing physical phase ϕ_μ that can appear in the EDMs' measurements.[6]

In the following, we assume that ϕ_μ is shifted by the gravity-mediated contribution as

$$\phi_\mu = \phi_\mu^{(0)} + \min\left\{\frac{m_{3/2}}{|B|}, \frac{\pi}{2}\right\}, \tag{16}$$

where the $\phi_\mu^{(0)}$ is the phase without the gravity-mediated contributions: $\phi_\mu^{(0)} = 0$ for scenario I and $\phi_\mu^{(0)} = \pi$ for scenarios II and III.

The leading SUSY contributions to the electron EDM come from the loop diagrams with chargino-sneutrino and neutralino-selectron exchange. They are well approximated as

$$\frac{d_e}{e} = \frac{\alpha_2}{4\pi}\frac{m_e t_\beta}{m_{\tilde{e}_L}^4}\frac{|M_2\mu|\sin\phi_\mu}{1+\varepsilon_e^2 t_\beta^2 + 2\varepsilon_e t_\beta\cos\phi_\mu} \times\left[F_2^{(e)}(x_{2L}, x_{\mu L}) + \frac{\alpha_Y|M_1|}{\alpha_2|M_2|}F_1^{(e)}(x_{1L}, x_{\mu L}, x_{1R}, x_{\mu R})\right], \tag{17}$$

with $t_\beta = \tan\beta$, $x_{1L/1R} = |M_1|^2/m_{\tilde{e}_{L/R}}^2$, $x_{2L/2R} = |M_2|^2/m_{\tilde{e}_{L/R}}^2$, and $x_{\mu L/\mu R} = |\mu|^2/m_{\tilde{e}_{L/R}}^2$. The loop functions $F_2^{(e)}$ and $F_1^{(e)}$ are defined in the Appendix. The coefficient ε_e stands for the $\tan\beta$-enhanced threshold corrections to the electron mass and it reads

$$\varepsilon_e = -\frac{3\alpha_2}{16\pi}\frac{|\mu M_2|}{m_{\tilde{e}_L}^2} \times\left[I_2^{(e)}(x_{2L}, x_{\mu L}) + \frac{\alpha_Y|M_1|}{\alpha_2|M_2|}I_1^{(e)}(x_{1L}, x_{\mu L}, x_{1R}, x_{\mu R})\right], \tag{18}$$

[5]In the small $m_{\rm SUSY}$ region in scenario I, there can be significant flavor mixings that may also be visible in FCNC processes. Also, in the calculations of the electron and nucleon EDMs, there can be significant contributions enhanced by heavy fermion masses through the sfermion mixings [13–15]. Since such parameter regions are anyway severely constrained by the flavor diagonal contributions, which we discuss in this section, we do not consider the flavor nondiagonal CP violation in the following analyses.

[6]The gravity-mediated contributions to the A term can be another source of the CP violation. Here we assume that their sizes are somehow controlled by the corresponding Yukawa couplings in order to avoid the color and charge breaking minimum. With this assumption, the dominant contribution to the EDM comes from the phase of the μ term thanks to the enhancement of $\tan\beta$.

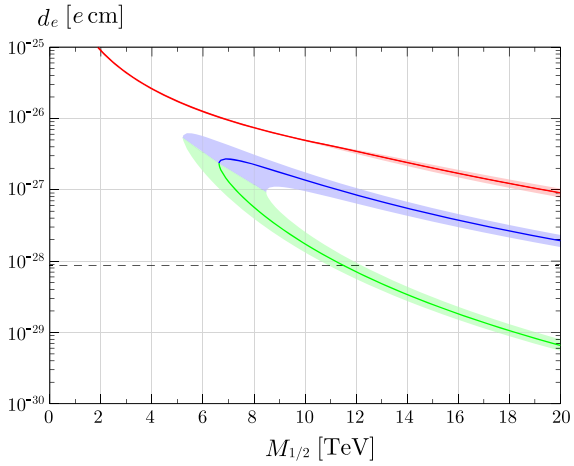

FIG. 6. The predicted electron EDMs as a function of $M_{1/2}$ in scenarios I (red), II (blue), and III (green). The dotted line shows the current experimental upper bound [43].

where the loop functions $I_2^{(e)}$ and $I_1^{(e)}$ are listed in the Appendix. In the limit of the common SUSY breaking masses, we find $F_2^{(e)}(1,1) = -5/24$, $F_1^{(e)}(1,1,1,1) = -1/24$, and $I_2^{(e)}(1,1) = 1$, $I_1^{(e)}(1,1,1,1) = -1/3$.

In Fig. 6, we show the expected values of the electron EDM, assuming the CP phase as Eq. (16). We find that the entire parameter region that explains the observed Higgs mass is disfavored by the EDM measurement in scenarios I and II. On the other hand, the constraint becomes milder for scenario III thanks to small $\tan\beta$ and small $\sin\phi_\mu \simeq m_{3/2}/|B|$. Although these predictions of the electron EDM contain O(1) uncertainty because the exact size of gravity-mediated contributions is unknown, it is plausible that the Higgs mass is explained in scenario III with $10\ \text{TeV} \lesssim M_{1/2} \lesssim 20\ \text{TeV}$, and the electron EDM is expected to be detected in the near-future experiments.

Since the SUSY spectrum is controlled by a common parameter $M_{1/2}$, one can obtain rigid predictions for the ratios between the electron EDM, quark EDMs, and quark Chromo-EDMs (CEDMs) irrespective of the actual size of the CP-violating phase. In this model, dominant contributions to the hadronic EDMs come from down-quark (C)EDMs, and they read

$$\frac{d_d}{e} = \frac{\alpha_3}{4\pi}\frac{m_d t_\beta}{m_{\tilde{d}_L}^4}\frac{|M_3\mu|\sin\phi_\mu}{1+\varepsilon_d^2 t_\beta^2 + 2\varepsilon_d t_\beta\cos\phi_\mu} \times\left[F_3^{(d)}(y_{3L}, y_{3R}) + \frac{\alpha_2|M_2|}{\alpha_3|M_3|}F_2^{(d)}(y_{2L}, y_{\mu L}) + \frac{\alpha_Y|M_1|}{\alpha_3|M_3|}F_1^{(d)}(y_{1L}, y_{\mu L}, y_{1R}, y_{\mu R})\right], \tag{19}$$

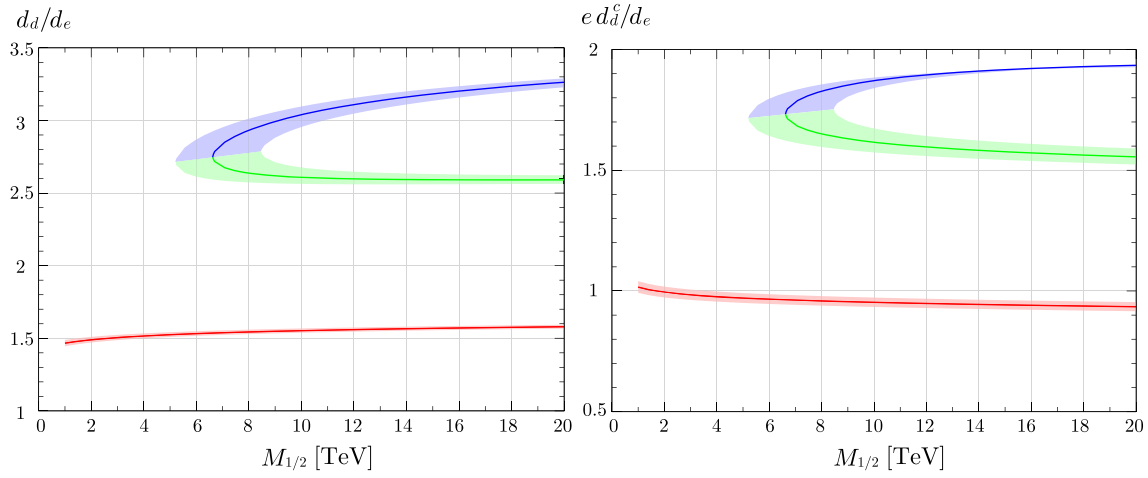

FIG. 7. Predicted ratios of down-quark EDM (left) and CEDM (right) to the electron EDM as a function of $M_{1/2}$ in scenarios I (red), II (blue), and III (green).

$$d_d^c = \frac{\alpha_3}{4\pi}\frac{m_d t_\beta}{m^4_{\tilde{d}_L}}\frac{|M_3\mu|\sin\phi_\mu}{1+\varepsilon_d^2 t_\beta^2 + 2\varepsilon_d t_\beta\cos\phi_\mu} \times\left[G_3^{(d)}(y_{3L},y_{3R}) + \frac{\alpha_2|M_2|}{\alpha_3|M_3|}G_2^{(d)}(y_{2L},y_{\mu L}) + \frac{\alpha_Y|M_1|}{\alpha_3|M_3|}G_1^{(d)}(y_{1L},y_{\mu L},y_{1R},y_{\mu R})\right], \quad (20)$$

where the $\tan\beta$-enhanced threshold corrections to down-quark mass are parametrized by

$$\varepsilon_d = \frac{\alpha_3}{3\pi}\frac{|\mu M_3|}{m^2_{\tilde{d}_L}}\left[I_3^{(d)}(y_{3L},y_{3R}) + \frac{\alpha_2|M_2|}{\alpha_3|M_3|}I_2^{(d)}(y_{2L},y_{\mu L}) + \frac{\alpha_Y|M_1|}{\alpha_3|M_3|}I_1^{(d)}(y_{1L},y_{\mu L},y_{1R},y_{\mu R})\right]. \quad (21)$$

Here, $y_{1L/1R} = |M_1|^2/m^2_{\tilde{d}_{L/R}}$, $y_{2L/2R} = |M_2|^2/m^2_{\tilde{d}_{L/R}}$, and $y_{\mu L/\mu R} = |\mu|^2/m^2_{\tilde{d}_{L/R}}$. The loop functions $F_i^{(d)}$, $G_i^{(d)}$, and $I_i^{(d)}$ $(i = 1, 2, 3)$ are defined in the Appendix. For the common SUSY breaking masses, the functions become $F^{(d)}_{\{1,2,3\}} = \{11/648, -7/24, -2/27\}$, $G^{(d)}_{\{1,2,3\}} = \{-11/216, -1/8, -5/18\}$, and $I^{(d)}_{\{1,2,3\}} = \{-11/48, -9/16, 1\}$. Similarly, the CP phase also generates the strange quark (C)EDMs, which are estimated as $d_s/d_d \simeq d_s^c/d_d^c \simeq m_s/m_d \simeq 18$, but their contributions to the hadronic EDMs are still uncertain [44]. These quark (C)EDMs are evaluated at the SUSY scale, and their values at the hadronic scale $\mu_H = 1$ GeV are obtained by the renormalization evolution [45].

From Eqs. (17), (19), and (20), the electron EDM and down-quark (C)EDMs are almost proportional to the imaginary part of the phase $\sin\phi_\mu$, and their ratios have rather weak dependence on the size of the phase. In scenarios I and II, the naive expectation of the phase can be $\mathcal{O}(1)$. However, this uncertainty becomes almost negligible once the size of the phase is restricted to satisfy the current experimental bound. In Fig. 7, we show the predicted ratios of the down-quark (C)EDMs to the electron EDM, with setting the CP phase to be small enough to satisfy the experimental bound. For $\cos\phi_\mu < 0$, the down-quark (C)EDMs are enhanced by the threshold corrections to the down-quark mass term, while the electron EDM is decreased. Therefore, the down-quark (C)EDMs can become relatively large in scenarios II and III.

The experimental sensitivities of the electron EDM [46–48] and the nucleon EDMs [49–53] are expected to be improved by several orders of magnitude in the next-generation experiments, and the measurements of these EDMs are essential to confirm or reject our model. The nucleon EDMs are induced by the quark (C)EDMs, and their contributions are estimated by using the QCD sum rules as follows [44,54][7]:

$$d_n = -0.20 d_u + 0.78 d_d + e(0.29 d_u^c + 0.59 d_d^c), \quad (22)$$

$$d_p = 0.78 d_u - 0.20 d_d + e(-1.2 d_u^c - 0.15 d_d^c). \quad (23)$$

Note, while the quark EDM contributions to the neutron EDM are well consistent with the recent result obtained by the lattice simulation [55], the quark CEDM contributions contain large theoretical uncertainties, and they should be fixed ultimately by the lattice QCD calculation. With the expressions of Eqs. (22) and (23), the sizes of nucleon EDMs are predicted as $d_n/d_e \simeq 1.8, 3.5, 3.0$ and

[7]This formulas are obtained with the assumption that the Peccei-Quinn symmetry works to suppress the contribution from the QCD θ term.

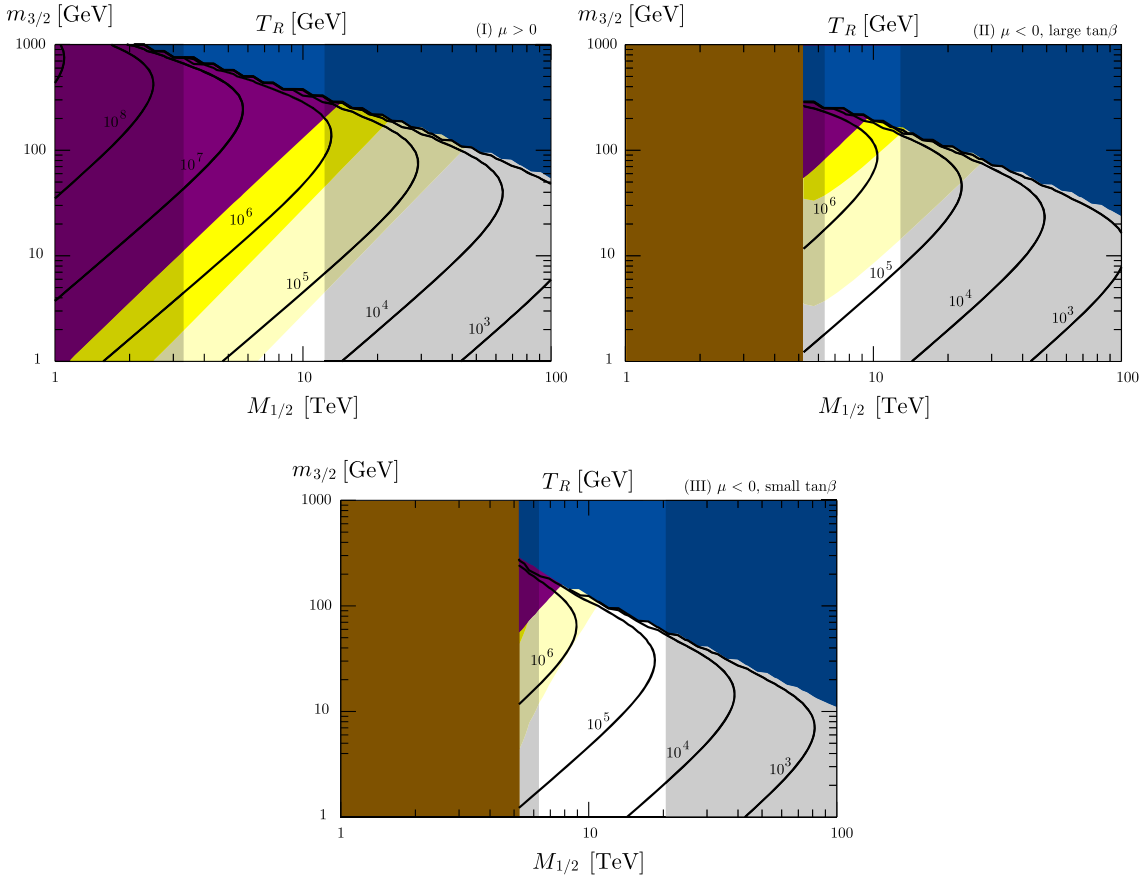

FIG. 8. Upper bounds on the reheating temperature T_R as functions of $M_{1/2}$ and $m_{3/2}$ in scenarios I (top left), II (top right), and III (bottom). Colored regions are excluded by the following conditions: gray, explanation of the Higgs mass; blue, overabundance of the gravitino dark matter relic density; brown, no EWSB minimum; purple, BBN constraints; yellow, no observation of the electron EDM, assuming $\phi_B = m_{3/2}/B$ (light yellow) and $\phi_B = 0.1 m_{3/2}/B$ (dark yellow).

$d_p/d_e \simeq -0.5, -0.9, -0.8$ for $M_{1/2} = 15$ TeV[8] in scenarios I, II, and III, respectively.

V. THERMALLY PRODUCED GRAVITINOS

As we have seen in earlier subsections, if most of the cold dark matter in our Universe consists of the gravitinos produced by the decay of other SUSY particles, scenarios I and II are disfavored by the BBN constraint and/or the EDM measurement. These constraints can be alleviated if the gravitino is much lighter than those expected by the calculation of the nonthermal production.

In the actual ultraviolet physics, it is nontrivial whether light gravitinos can be realized with satisfying the boundary conditions Eqs. (3) and (5) at the GUT scale. For example, the models using the gaugino mediation are primary candidates of our UV complete model, but the gravitino mass has lower bounds depending on the number of extra dimensions [56].

Here, we leave aside such difficulty of the model building and discuss phenomenological implications of the model with much lighter gravitinos. In this case, nonthermally produced gravitinos cannot be the main constituent of the cold dark matter. The gravitinos can be also produced thermally by scattering processes with particles in the thermal bath. The resultant abundance is approximately proportional to the reheating temperature after the inflation T_R, and it reads [42]

$$\Omega_{\tilde{G}}^{\rm th} h^2 \simeq 0.41 \left(\frac{m_{3/2}}{100\ \text{GeV}}\right)^{-1} \left(\frac{M_{1/2}}{10\ \text{TeV}}\right)^2 \left(\frac{T_R}{10^7\ \text{GeV}}\right). \tag{24}$$

Requiring that the total gravitino abundance is smaller than the observed dark matter abundance $\Omega_{\tilde{G}}^{\rm NT} + \Omega_{\tilde{G}}^{\rm th} < \Omega_c$, we obtain the upper bounds on the reheating temperature.

In Fig. 8, we show the upper bounds on the reheating temperatures in the $(M_{1/2}, m_{3/2})$ plane for scenarios I, II, and III. The gray shaded regions cannot explain the Higgs mass even if the top mass is chosen in the range of $M_t = 173.3 \pm 2$ GeV. The gravitino abundance exceeds

[8]Since $M_{1/2}$ dependence of d_n/d_e and d_p/d_e is not so significant, we have shown values at the sample point.

the observed dark matter abundance in the blue regions. The purple regions are excluded by the BBN constraints, which imply $\tau_{\tilde{\tau}} > 100$ sec, and the correct EWSB minimum cannot be obtained in the brown regions. The yellow regions are disfavored by the electron EDM constraint, assuming $\phi_B = m_{3/2}/B$ (light yellow) and $\phi_B = 0.1 m_{3/2}/B$ (dark yellow). Apart from the calculation of the Higgs mass, we choose $M_t = 171.3$ GeV in this plot, and its precise value is less sensitive to the predictions of the reheating temperature and other constraints.

We find that the gravitino mass should be less than about 10 GeV in scenarios I and II to suppress the SUSY contributions to the electron EDM. With this small gravitino mass, the reheating temperature becomes relatively low, less than about 10^5 GeV. In scenario III, the constraint from the EDM becomes weaker, and the upper bound on the reheating temperature increases to 10^6 GeV.

VI. SUMMARY AND DISCUSSION

In this paper, we have discussed a model where the SUSY breaking effects are mediated only to the gaugino mass terms at the leading order as a simple solution for the SUSY flavor and CP problems. The gravitino mass should be smaller than other SUSY breaking parameters to suppress the gravity-mediated contributions, which are the main sources of flavor and CP violation in our model. Thus, in the presence of the R-parity conservation, the gravitino becomes a good candidate of the cold dark matter in our Universe.

We have carefully examined the RG running of the B parameter and have found that the parameter region with small $\tan\beta$ appears as the SUSY scale increases. Thanks to the smallness of $\tan\beta$, the SUSY breaking scale to explain the Higgs boson mass is pushed up, and, particularly, the NLSP right-handed stau mass is increased. Then, since the lifetime of the NLSP staus is shortened in this parameter region, the entire observed dark matter abundance can be explained by the gravitinos produced by the decay of other SUSY particles without destroying the successful predictions of the standard BBN scenario.

Since the B parameter is relatively small compared to other SUSY breaking parameters, it is affected by the small gravity-mediated contributions. Thus, we expect non-negligible SUSY contributions to the electron and nucleon EDMs. We have found that the naively expected sizes of the electron EDM are on the edge of the current experimental limit, and it should be checked in the near-future experiments. In particular, the ratios of the nucleon EDMs to the electron EDM become the key ingredients for the discrimination of our model with others.

Our model is very predictive, and the entire SUSY mass spectrum is fixed if the top Yukawa coupling is measured precisely and the theoretical errors in the Higgs mass calculation are reduced. Then it is important to measure the mass of the lightest MSSM SUSY particle, right-handed stau at the future collider experiments such as in the future 100 TeV hadron colliders [57,58]. We expect that our model will be tested by the combination of the future collider and EDM experiments.

Finally, we comment on the UV theory of the model. In this analysis, the μ term is assumed to be a fundamental parameter which is comparable to the SUSY scale and tuned to generate the correct electroweak scale. Also, the gravitino mass is treated as a free parameter. To understand the whole picture of our model, it is desirable to construct the UV model which explains the origin of the μ term and predicts the preferable gravitino mass.

ACKNOWLEDGMENTS

This work is supported by JSPS KAKENHI Grant-in-Aid for Scientific Research (B) (Grant No. 15H03669 [R. K.]) and MEXT Grant-in-Aid for Scientific Research on Innovative Areas (Grant No. 25105011 [R. K.]). We would like to thank Kazunori Kohri for discussions.

APPENDIX: LOOP FUNCTIONS

We list the loop functions relevant to the calculation of EDMs:

$$
\begin{aligned}
F_1^{(e)}(x_{1L},x_{\mu L},x_{1R},x_{\mu R}) &= \frac{1}{4}D_0(x_{1L},x_{\mu L}) - \frac{x_{1R}^2}{2x_{1L}^2}D_0(x_{1R},x_{\mu R}) \\
&\quad - \frac{x_{1R}}{2x_{1L}}E_0(x_{1L},x_{1R}), \\
F_2^{(e)}(x_{2L},x_{\mu L}) &= -\frac{1}{2}D_1(x_{2L},x_{\mu L}) - \frac{1}{4}D_0(x_{2L},x_{\mu L}), \\
F_1^{(d)}(y_{1L},y_{\mu L},y_{1R},y_{\mu R}) &= \frac{y_{1R}}{54y_{1L}}E_0(y_{1L},y_{1R}) \\
&\quad - \frac{1}{36}D_0(y_{1L},y_{\mu L}) \\
&\quad - \frac{y_{1R}^2}{18y_{1L}^2}D_0(y_{1R},y_{\mu R}), \\
F_2^{(d)}(y_{2L},y_{\mu L}) &= -\frac{1}{2}D_1(y_{2L},y_{\mu L}) + \frac{1}{4}D_0(y_{2L},y_{\mu L}), \\
F_3^{(d)}(y_{3L},y_{3R}) &= -\frac{4y_{3R}}{9y_{3L}}E_0(y_{3L},y_{3R}), \\
G_1^{(d)}(y_{1L},y_{\mu L},y_{1R},y_{\mu R}) &= -\frac{y_{1R}}{18y_{1L}}E_0(y_{1L},y_{1R}) \\
&\quad + \frac{1}{12}D_0(y_{1L},y_{\mu L}) \\
&\quad + \frac{y_{1R}^2}{6y_{1L}^2}D_0(y_{1R},y_{\mu R}), \\
G_2^{(d)}(y_{2L},y_{\mu L}) &= \frac{3}{4}D_0(y_{2L},y_{\mu L}), \\
G_3^{(d)}(y_{3L},y_{3R}) &= -\frac{y_{3R}}{6x_{3L}}E_0(y_{3L},y_{3R}) \\
&\quad + \frac{3y_{3R}}{2y_{3L}}E_1(y_{3L},y_{3R}).
\end{aligned}
\tag{A1}
$$

Here, we define

$$D_i(x,y) = \frac{f_i(x) - f_i(y)}{x-y}, \qquad E_i(x,y) = \frac{x f_i(x) - y f_i(y)}{x-y}, \tag{A2}$$

for $i = 1, 2$ and

$$f_0(x) = \frac{1 - x^2 + 2x\log x}{(1-x)^3}, \qquad f_1(x) = \frac{3 - 4x + x^2 + 2\log x}{(1-x)^3}. \tag{A3}$$

In the limit of degenerate arguments, we obtain $D_0(1,1) = -1/6$, $D_1(1,1) = 1/2$, $E_0(1,1) = 1/6$, and $E_1(1,1) = -1/6$.

The following functions are used to calculate threshold corrections to the electron and down-quark masses,

$$\begin{aligned}
I_1^{(e)}(x_{1L}, x_{\mu L}, x_{1R}, x_{\mu R}) &= -\frac{4x_{1R}}{3x_{1L}} H_2(x_{1R}, x_{\mu R}) + \frac{2}{3} H_2(x_{1L}, x_{\mu L}) + \frac{4}{3} H_2(x_{1L}, x_{1L}/x_{1R}), \\
I_2^{(e)}(x_{2L}, x_{\mu L}) &= -2H_2(x_{2L}, x_{\mu L}), \\
I_1^{(d)}(y_{1L}, y_{\mu L}, y_{1R}, y_{\mu R}) &= \frac{y_{1R}}{4y_{1L}} H_2(y_{1R}, y_{\mu R}) + \frac{1}{8} H_2(y_{1L}, y_{\mu L}) + \frac{1}{12} H_2(y_{1L}, y_{1L}/y_{1R}), \\
I_2^{(d)}(y_{2L}, y_{\mu L}) &= \frac{9}{8} H_2(y_{2L}, y_{\mu L}), \\
I_3^{(d)}(y_{3L}, y_{3R}) &= -2H_2(y_{3L}, y_{3L}/y_{3R}),
\end{aligned} \tag{A4}$$

where

$$H_2(x,y) = \frac{x\log x}{(1-x)(x-y)} + \frac{y\log y}{(y-1)(x-y)}, \tag{A5}$$

and the function becomes $H_2(1,1) = -1/2$ for the degenerate arguments.

[1] M. Ibe, S. Matsumoto, T. T. Yanagida, and N. Yokozaki, J. High Energy Phys. 03 (2013) 078.
[2] P. Draper, G. Lee, and C. E. M. Wagner, Phys. Rev. D **89**, 055023 (2014).
[3] T. Hahn, S. Heinemeyer, W. Hollik, H. Rzehak, and G. Weiglein, arXiv:1404.0186.
[4] E. Bagnaschi, G. F. Giudice, P. Slavich, and A. Strumia, J. High Energy Phys. 09 (2014) 092.
[5] M. Ibe and T. T. Yanagida, Phys. Lett. B **709**, 374 (2012).
[6] M. Ibe, S. Matsumoto, and T. T. Yanagida, Phys. Rev. D **85**, 095011 (2012).
[7] A. Arvanitaki, N. Craig, S. Dimopoulos, and G. Villadoro, J. High Energy Phys. 02 (2013) 126.
[8] N. Arkani-Hamed, A. Gupta, D. E. Kaplan, N. Weiner, and T. Zorawski, arXiv:1212.6971.
[9] G. F. Giudice, M. A. Luty, H. Murayama, and R. Rattazzi, J. High Energy Phys. 12 (1998) 027.
[10] N. Arkani-Hamed and S. Dimopoulos, J. High Energy Phys. 06 (2005) 073.
[11] J. D. Wells, Phys. Rev. D **71**, 015013 (2005).
[12] L. J. Hall and Y. Nomura, J. High Energy Phys. 01 (2012) 082.
[13] T. Moroi and M. Nagai, Phys. Lett. B **723**, 107 (2013).
[14] D. McKeen, M. Pospelov, and A. Ritz, Phys. Rev. D **87**, 113002 (2013).
[15] W. Altmannshofer, R. Harnik, and J. Zupan, J. High Energy Phys. 11 (2013) 202.
[16] J. Hisano, S. Matsumoto, M. Nagai, O. Saito, and M. Senami, Phys. Lett. B **646**, 34 (2007).
[17] L. Randall and R. Sundrum, Nucl. Phys. **B557**, 79 (1999).
[18] M. Dine, W. Fischler, and M. Srednicki, Nucl. Phys. **B189**, 575 (1981).
[19] S. Dimopoulos and S. Raby, Nucl. Phys. **B192**, 353 (1981).
[20] D. E. Kaplan, G. D. Kribs, and M. Schmaltz, Phys. Rev. D **62**, 035010 (2000).
[21] Z. Chacko, M. A. Luty, A. E. Nelson, and E. Ponton, J. High Energy Phys. 01 (2000) 003.
[22] J. L. Feng, A. Rajaraman, and F. Takayama, Phys. Rev. Lett. **91**, 011302 (2003).
[23] J. L. Feng, A. Rajaraman, and F. Takayama, Phys. Rev. D **68**, 063504 (2003).
[24] J. R. Ellis, A. B. Lahanas, D. V. Nanopoulos, and K. Tamvakis, Phys. Lett. **134B**, 429 (1984).

[25] J. R. Ellis, C. Kounnas, and D. V. Nanopoulos, Nucl. Phys. **B241**, 406 (1984); **B247**, 373 (1984); Phys. Lett. **143B**, 410 (1984); J. R. Ellis, K. Enqvist, and D. V. Nanopoulos, Phys. Lett. **147B**, 99 (1984).
[26] G. F. Giudice and A. Strumia, Nucl. Phys. **B858**, 63 (2012).
[27] D. Buttazzo, G. Degrassi, P. P. Giardino, G. F. Giudice, F. Sala, A. Salvio, and A. Strumia, J. High Energy Phys. 12 (2013) 089.
[28] S. Chatrchyan *et al.* (CMS Collaboration), Eur. Phys. J. C **74**, 2758 (2014).
[29] V. M. Abazov *et al.* (D0 Collaboration), Phys. Rev. Lett. **113**, 032002 (2014).
[30] T. A. Aaltonen *et al.* (CDF Collaboration), Phys. Rev. D **90**, 091101 (2014).
[31] B. C. Allanach, Comput. Phys. Commun. **143**, 305 (2002).
[32] G. Aad *et al.* (ATLAS and CMS Collaborations), Phys. Rev. Lett. **114**, 191803 (2015).
[33] T. Asaka, K. Hamaguchi, and K. Suzuki, Phys. Lett. B **490**, 136 (2000).
[34] K. Griest and D. Seckel, Phys. Rev. D **43**, 3191 (1991).
[35] J. R. Ellis, T. Falk, K. A. Olive, and M. Srednicki, Astropart. Phys. **13**, 181 (2000); **15**, 413(E) (2001).
[36] C. F. Berger, L. Covi, S. Kraml, and F. Palorini, J. Cosmol. Astropart. Phys. 10 (2008) 005.
[37] M. Ratz, K. Schmidt-Hoberg, and M. W. Winkler, J. Cosmol. Astropart. Phys. 10 (2008) 026.
[38] M. Endo, K. Hamaguchi, and K. Nakaji, J. High Energy Phys. 11 (2010) 004.
[39] P. A. R. Ade *et al.* (Planck Collaboration), Astron. Astrophys. **594**, A13 (2016).
[40] J. L. Feng, S. f. Su, and F. Takayama, Phys. Rev. D **70**, 063514 (2004).
[41] M. Kawasaki, K. Kohri, and T. Moroi, Phys. Rev. D **71**, 083502 (2005).
[42] M. Kawasaki, K. Kohri, T. Moroi, and A. Yotsuyanagi, Phys. Rev. D **78**, 065011 (2008).
[43] J. Baron *et al.* (ACME Collaboration), Science **343**, 269 (2014).
[44] J. Hisano, J. Y. Lee, N. Nagata, and Y. Shimizu, Phys. Rev. D **85**, 114044 (2012).
[45] G. Degrassi, E. Franco, S. Marchetti, and L. Silvestrini, J. High Energy Phys. 11 (2005) 044.
[46] Y. Sakemi *et al.*, J. Phys. Conf. Ser. **302**, 012051 (2011).
[47] D. M. Kara, I. J. Smallman, J. J. Hudson, B. E. Sauer, M. R. Tarbutt, and E. A. Hinds, New J. Phys. **14**, 103051 (2012).
[48] D. Kawall, J. Phys. Conf. Ser. **295**, 012031 (2011).
[49] F. M. Piegsa, Phys. Rev. C **88**, 045502 (2013).
[50] K. Matsuta *et al.*, AIP Conf. Proc. **1560**, 152 (2013).
[51] A. P. Serebrov *et al.*, Phys. Rev. C **92**, 055501 (2015).
[52] Y. K. Semertzidis (Storage Ring EDM Collaboration), arXiv:1110.3378.
[53] A. Lehrach, B. Lorentz, W. Morse, N. Nikolaev, and F. Rathmann, arXiv:1201.5773.
[54] J. Hisano, D. Kobayashi, W. Kuramoto, and T. Kuwahara, J. High Energy Phys. 11 (2015) 085.
[55] T. Bhattacharya, V. Cirigliano, R. Gupta, H. W. Lin, and B. Yoon, Phys. Rev. Lett. **115**, 212002 (2015).
[56] W. Buchmuller, K. Hamaguchi, and J. Kersten, Phys. Lett. B **632**, 366 (2006).
[57] T. Cohen, T. Golling, M. Hance, A. Henrichs, K. Howe, J. Loyal, S. Padhi, and J. G. Wacker, J. High Energy Phys. 04 (2014) 117.
[58] J. L. Feng, S. Iwamoto, Y. Shadmi, and S. Tarem, J. High Energy Phys. 12 (2015) 166.